Transients Caused by Uncontrolled and Controlled Switching of Circuit Breakers

Ivo Uglešić, Božidar Filipović-Grčić and Srećko Bojić

***Abstract*—This paper describes transients caused by uncontrolled and controlled switching of high-voltage circuit breakers. Inrush currents due to shunt reactor energization were analyzed. Switching-off, energization and auto-reclosure of unloaded 400 kV transmission line is presented. Transient recovery voltage and voltage distribution between breaking chambers of circuit breaker are investigated. Calculation models were developed in EMTP-RV software and some field measurements are presented. Results show that controlled switching significantly reduces inrush currents and suppresses switching overvoltages.**

***Index Terms*—circuit breaker, controlled and uncontrolled switching, shunt reactor, inrush current, no-load 400 kV transmission line, simulations, measurements.**

I. Introduction

UNCONTROLLED switching of shunt reactors, shunt capacitors and transmission lines may cause severe transients such as high overvoltages or high inrush currents [1]. Conventional countermeasures such as pre-insertion resistors, damping reactors or resistors, or arresters are used to limit the magnitude and effect of the switching transients, after they have occurred. In addition, system and equipment insulation may be upgraded to withstand the stresses. These methods, however, may be inefficient, unreliable or expensive, and do not treat the root of the problem [2].

Controlled switching is a method for eliminating harmful transients via time controlled switching operations. Closing or opening commands to the circuit breaker are delayed in such a way that switching will occur at the optimum time instant related to the voltage phase angle. Controlled switching has become an economical substitute for a closing resistor and is commonly used to reduce switching surges. The number of installations using controlled switching has increased rapidly due to satisfactory service performance since the late 1990s [3]. Currently, it is often specified for shunt capacitor and shunt reactor banks because it can provide several economic benefits such as elimination of closing resistors and extension of a circuit breaker nozzle and contact maintenance interval. It also provides various technical benefits such as improved power quality and suppression of transients in transmission and distribution systems [4].

This paper describes switching transients caused by uncontrolled and controlled switching of circuit breaker. Switching of shunt reactor and no-load transmission line is analyzed using EMTP-RV software. Field measurements are presented and compared with simulation results.

II. Transients Caused By Switching of Shunt Reactor

The function of shunt reactors in transmission networks is to consume the excess reactive power generated by overhead lines under low-load conditions, and thereby stabilize the system voltage. They are quite often switched in and out on a daily basis, following the load situation in the system. Energization of a shunt reactor may cause inrush currents with high asymmetry and long time constants. The actual magnitude of the inrush current is quite dependent on the range of linearity of the reactor core and on the time instant of circuit breaker pole operation with respect to the reference signal. Switching operations at unfavorable instants can cause currents that may reach high magnitudes and have long time constants. At shunt reactors with solidly grounded neutral, unsymmetrical currents cause zero-sequence current flow which can activate zero-sequence current relays [5].

A. Model Description

The inrush currents due to energization of 150 MVAr shunt reactor in 110 kV network have been observed. Both uncontrolled and controlled circuit breaker switching is simulated. Shunt reactor manufacturer data are shown in Table I.

TABLE I 150 MVA Shunt Rector Data

Rated power	150 MVAr
Rated frequency	50 Hz
Rated voltage	110 kV
Rated current	787 A
Core type	Five limb
Total losses (at 110 kV)	363 kW
Impedance in saturation	38 Ω
Zero sequence impedance	80,7 Ω per phase
Stationary magnetic flux	1,32 T
Capacitance of winding to ground	1,36 nF per phase

Calculation of inrush currents requires an adequate modeling of the reactor nonlinear flux-current curve. The nonlinearity is caused by the magnetizing characteristics of the shunt reactor iron core. Recorded RMS voltage-current curve

I. Uglešić and B. Filipović-Grčić are with the University of Zagreb, Faculty of Electrical Engineering and Computing, Unska 3, 10000 Zagreb, Croatia (e-mail: ivo.uglesic@fer.hr; bozidar.filipovic-grcic@fer.hr).

S. Bojić is with Energy Institute Inc., Ul. grada Vukovara 37, 10000 Zagreb, Croatia (e-mail: srecko.bojic@ie-zagreb.hr).

obtained from manufacturer test data is converted into instantaneous flux-current saturation curve (Fig. 1) which is used in the nonlinear inductance model in EMTP-RV [6] and approximated with two segments (linear area A'-B', below knee of the saturation curve and saturation area B'-C').

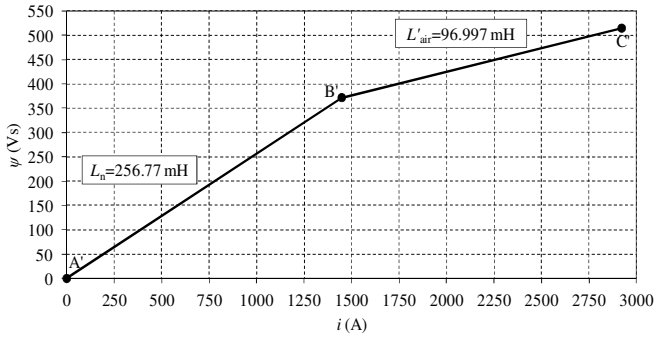

Fig. 1. Instantaneous flux-current saturation curve of 150 MVAr shunt reactor

Model for analysis of shunt reactor switching in EMTP-RV is shown in Figure 2.

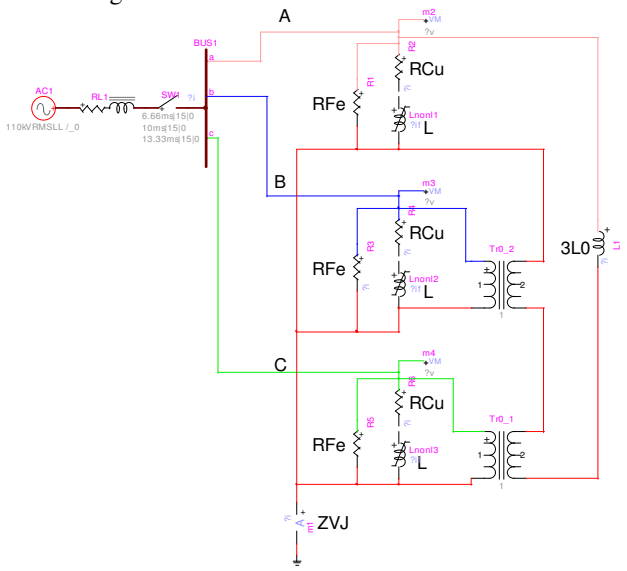

Fig. 2. Model for analysis of shunt reactor switching in EMTP-RV

Each phase of a three phase shunt reactor is modeled as a nonlinear inductance with serially connected resistance R_{Cu}=146.5 mΩ, representing copper losses and parallel connected R_{Fe}=133.3 kΩ, representing iron losses. Magnetic coupling among the three star connected phases is represented with zero sequence inductance L_0=257 mH which provides a path for the zero sequence current [7]. Equivalent 110 kV network is represented with positive (R_1=265 mΩ, L_1=7 mH) and zero (R_0=216 mΩ, L_0=5,7 mH) sequence impedances, determined from single-phase and three-phase short circuit currents: $I_{sc1} = 33.8\,kA\angle -83.1^\circ$, $I_{sc3} = 31.7\,kA\angle -83.1^\circ$.

B. Uncontrolled Energization

By uncontrolled energization the following instants of pole closing were considered: t_A=15 ms, t_B=13 ms and t_C=17 ms. Figures 3 and 4 show shunt reactor voltages and currents, respectively. The highest inrush current happened when switching occurs at an instant near the voltage zero-crossing in phase A, since it results with the maximum DC component of current.

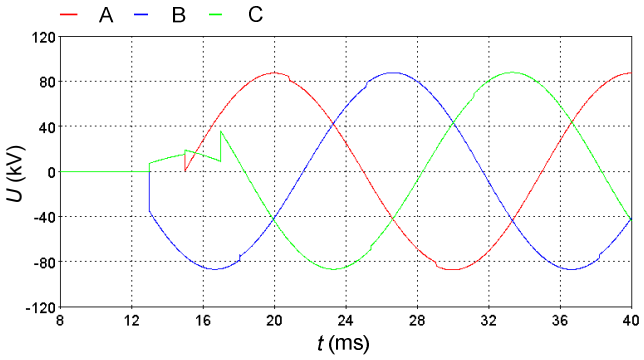

Fig. 3. Shunt reactor voltages in case of reactor uncontrolled energization

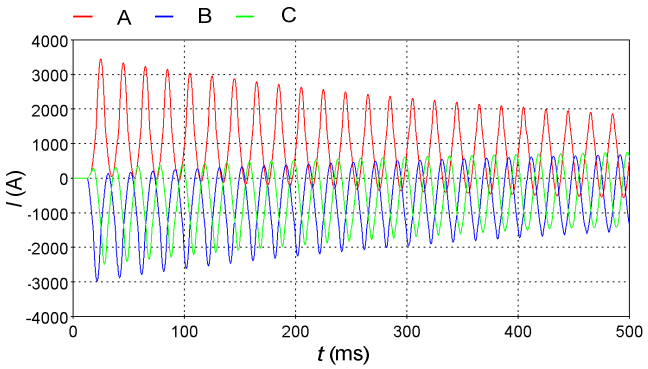

Fig. 4. Shunt reactor currents in case of reactor uncontrolled energization: I_{Amax}= 3455 A (3.10 p.u.), I_{Bmax}=-2982 A (2.68 p.u.), I_{Cmax}=-2494 A (2.24 p.u.)

Conducted simulation shows that transient inrush current with amplitude of 3.10 p.u. and high DC component can last up to 3.5 seconds (Fig. 5). This could cause difficulties, such as unwanted operation of the overcurrent relay protection.

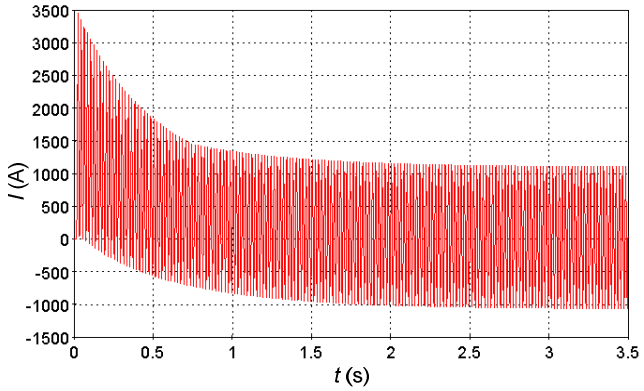

Fig. 5. Shunt reactor current in phase A in case of reactor uncontrolled energization

Zero sequence current occurs in case of uncontrolled reactor energization (Fig. 6) as a consequence of asymmetry. This may cause the false operation of relay protection, used for detecting single phase-to-ground faults.

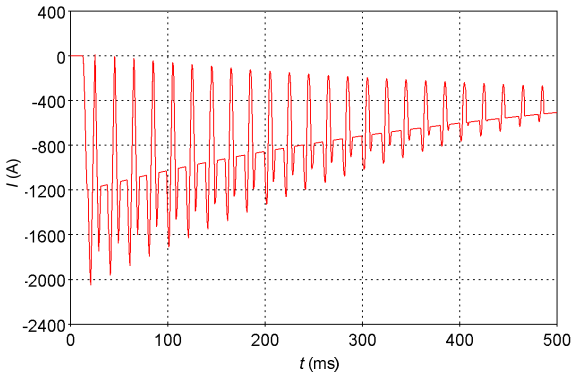

Fig. 6. Zero-sequence current in case of reactor uncontrolled energization I_{max}=-2052 A (1.84 p.u.)

C. Controlled Energization

Figures 7 and 8 show shunt reactor voltages and currents in case of controlled energization at optimum instants of circuit breaker poles closing at peak voltages (t_A=10 ms, t_B=6.66 ms and t_C=13.33 ms).

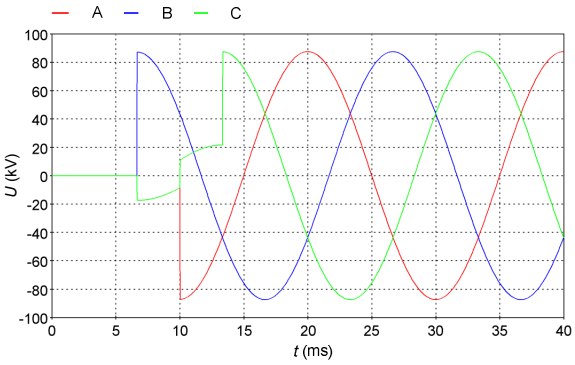

Fig. 7. Shunt reactor voltages in case of reactor controlled energization

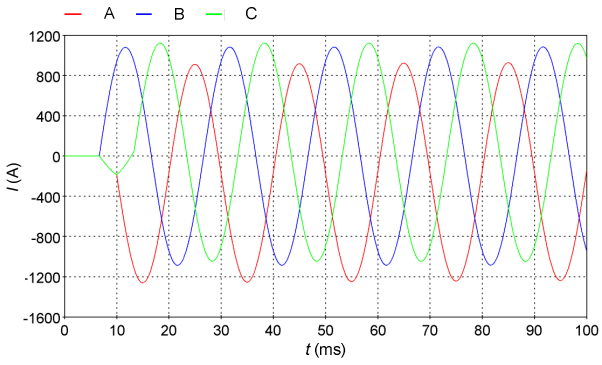

Fig. 8. Shunt reactor currents in case of reactor controlled energization, I_{Amax}=-1260 A (1.13 p.u.), I_{Bmax}=1090 A (0.98 p.u.), I_{Cmax}=1123 A (1.01 p.u.)

The current in phase A (Fig. 8) is slightly larger than in the other two phases, due to the appearance of the DC component, which is caused by initial magnetic flux in the core limb of that phase at the moment of energization. This initial magnetic flux is a part of a magnetic flux from the phase B, which is firstly being switched on (Fig. 9). The final distribution of the magnetic flux in the reactor core is shown in Fig. 10. Due to the air gaps utilized in shunt reactor core there are no severe saturation effects [8].

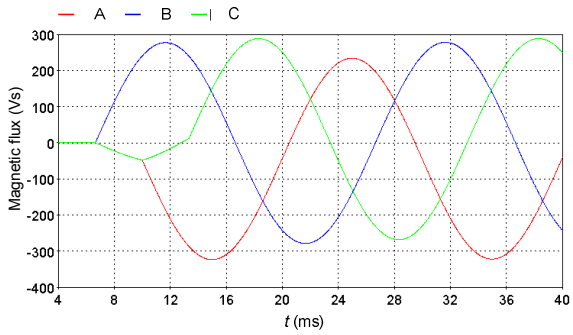

Fig. 9. Magnetic flux in case of reactor controlled energization

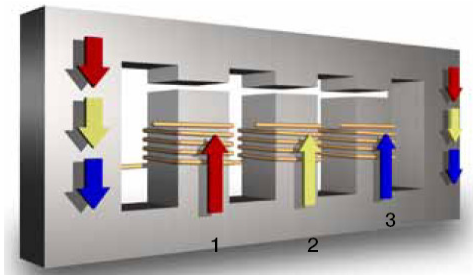

Fig. 10. The distribution of the magnetic flux in the five limb core of shunt reactor - phase A (1), B (2) and C (3)

Conducted simulation shows that amplitudes and DC components of inrush current (Fig 11) and zero-sequence current (Fig 12) are significantly lower in case of controlled switching. As a consequence, successfuly controlled switching reduces the mechanical and electromagnetic stresses of the high voltage equipment and also prevents the unwanted operation of relay protection.

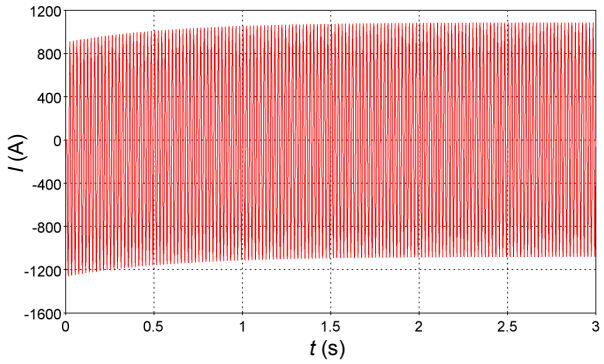

Fig. 11. Shunt reactor current in phase A

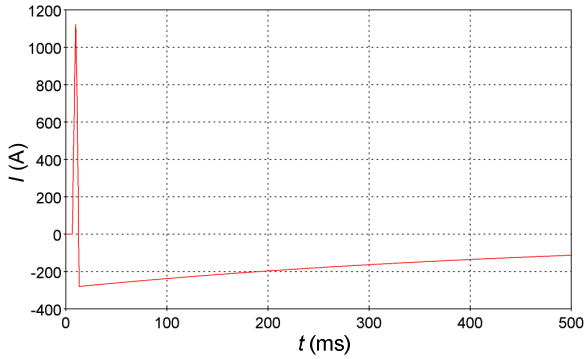

Fig. 11. Zero-sequence current, I_{zmax}=1122 A (1.01 p.u.)

III. Transients Caused By Switching Unloaded 400 kV Transmission Line

A. Measurements of switching transients

The measurements of switching transients caused by uncontrolled switching of the 231 km long line were performed. Figures 12 and 13 show recorded TRV and phase voltages on line side in case of switching-off line by circuit breaker equipped with grading capacitors.

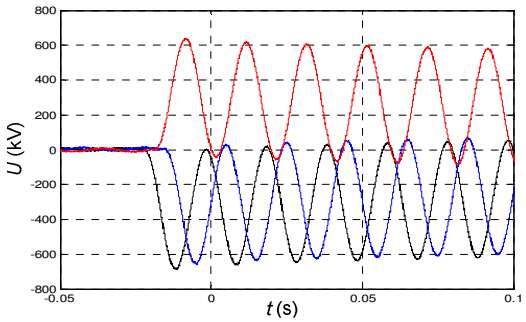

Fig. 12. Recorded TRV in case of regular switching-off: U_{L1}= -686 kV (2.08 p.u.),U_{L2}=-657 kV (1.99 p.u.), U_{L3}=641 kV (1.94 p.u.)

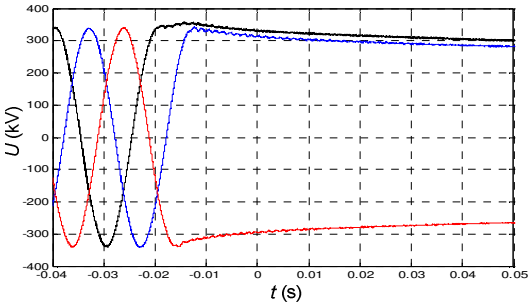

Fig. 13. Recorded phase voltages on line-side after regular switching-off U_{L1}=360 kV (1.09 p.u.), U_{L2}= 351 kV (1.06 p.u.), U_{L3}= -348 kV (1.06 p.u.)

B. Model Description

Model for the analysis of switching the 231 km long 400 kV unloaded transmission line [9] is shown in Fig. 14.

The equipment in high voltage substation was represented by surge capacitances, whereas transmission lines, busbars and connecting leads by a frequency depending line model [10]. The phase transpositions of the transmission lines have been taken into account. The MO surge arresters were modeled with nonlinear *U-I* curves for switching overvoltages.

The model of CB with two breaking chambers for switching the transmission line 2 is shown in Fig. 15.

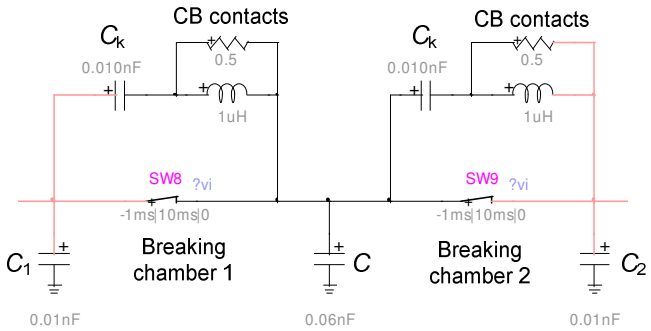

Fig .15. Model of circuit breaker with two braking chambers

The capacitance between the open contacts of breaking chambers is 10 pF and inherent earth capacitances were taken into account as depicted in Fig. 15.

The equivalent networks were represented with a voltage source in series with sequences impedances, which are obtained from short circuit currents in case of switching state prior to a fault (Table II).

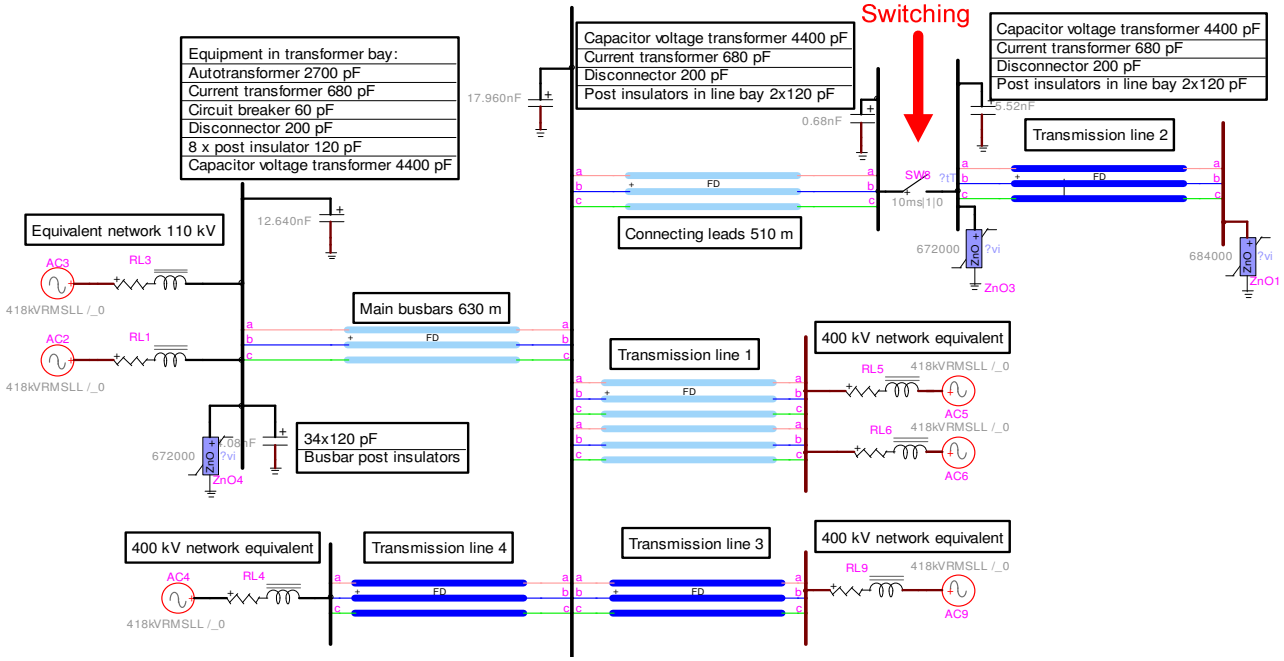

Fig. 14. Model for analyzes of circuit breaker switching no-load 400 kV transmission line in EMTP-RV

TABLE II
SHORT CIRCUIT CURRENTS IN 400 KV SUBSTATION

Connections:	I_{3ph} (kA/°)	I_{1ph} (kA/°)
Transmission line 1 (86.3 km)	3.4/-85.5	2.4/-82.2
	3.4/-85.5	2.4/-82.2
Transmission line 2 (231 km)	2.4/84.8	1.8/-80.0
Transmission line 3 (91.5 km)	4.1/-84.9	3.3/-79.9
Transmission line 4 (152 km)	3.9/84.9	3.0/-80.1
Power transformer TR 1 (400/110 kV)	1.2/-81.5	1.3/-84.8
Power transformer TR 2 (400/110 kV)	1.1/-81.5	1.3/-84.8
Total:	19.5/-84.7	15.6/-81.6

C. *Switching-off unloaded 400 kV transmission line*

When an unloaded line is regularly switched-off the electric arc distinguishing occurs at current natural zero-crossing. Fig. 16 shows phase voltages on line-side after regular switching-off. Voltage is highest in the phase which is firstly switched-off due to the electromagnetic coupling of the other phases and due to Ferranti effect.

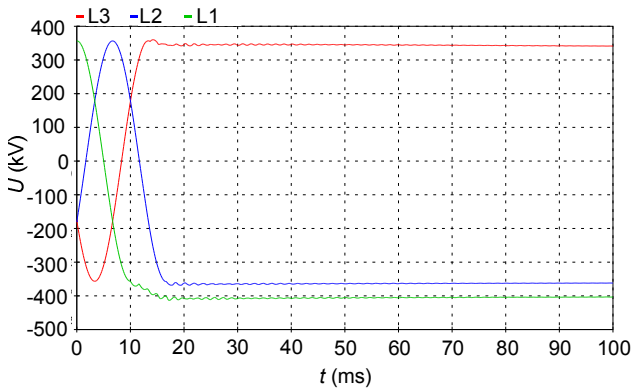

Fig. 16. Phase voltages on line-side after regular switching-off

Since the capacitor voltage transformers are installed on both sides of the line the discharging of trapped charge is slow. Such discharging depends on weather conditions, mainly on humidity. So, the trapped charge has a very significant influence on CB transient recovery voltage (Fig. 17).

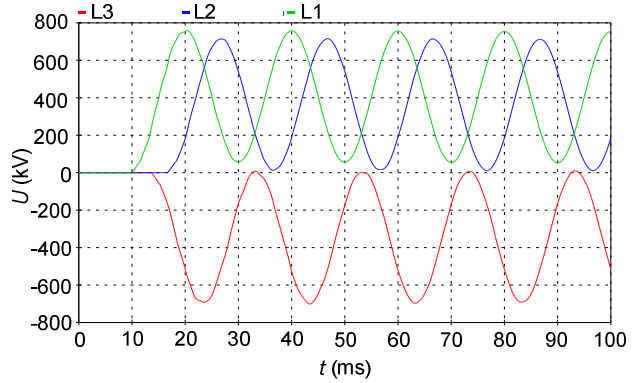

Fig. 17. TRV in case of regular switching-off: U_{L1}=758 kV (2.32 p.u.), U_{L2}=713 kV (2.18 p.u.), U_{L3}=692 kV (2.12 p.u.)

Besides the peak value of TRV the voltage distribution between breaking chambers is very important for CB dielectric stresses during switching operations. Simulation results show pretty unequal voltage distribution between breaking chambers in phase L1 where the maximum peak of TRV occurs (Fig. 18).

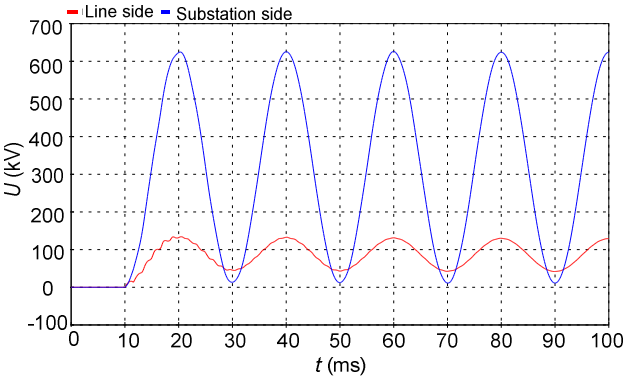

Fig. 18. Distribution of CB recovery voltage between breaking chambers

The voltage distribution between the breaking chambers could be improved by installing the grading capacitors, which are especially important in cases when switching-off relatively long lines. Further analyses show the influence of grading capacitors of 500 pF on voltage distribution. Simulation results show significant improvement of voltage distribution and reduction of TRV amplitude (Fig. 19).

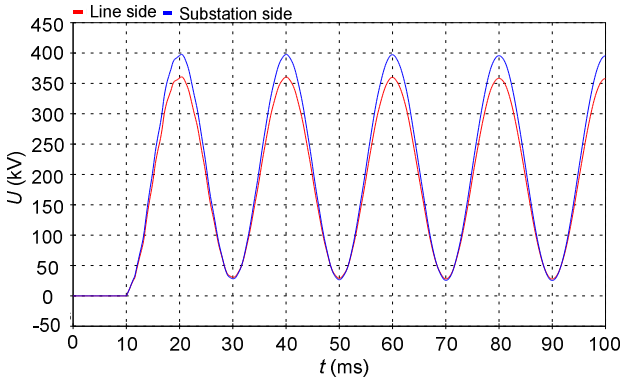

Fig. 19. Distribution of CB recovery voltage between breaking chambers in case with grading capacitors

Fig. 20 shows the comparison of calculated TRV peak values in cases with and without grading capacitors.

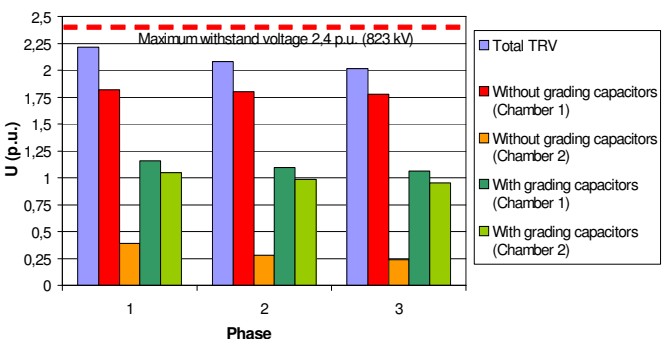

Fig. 20. Calculated TRV when switching-off unloaded 400 kV line

The CB should withstand the maximum voltage of 823 kV (2.4 p.u.) across the open contacts [11]. Compared to this, the computed value of recovery voltage is only 10 % smaller (758 kV/2.2 p.u.). However, the greatest part (nearly 80 %) of TRV stresses the breaking chamber closer to the substation.

D. Energization of unloaded 400 kV transmission line without trapped charge

Energization and auto-reclosure of long transmission lines can cause undesirable overvoltages in the transmission network, so special overvoltage mitigation measures are employed to meet the insulation coordination considerations. The most common practice has been to use metal-oxide surge arresters and circuit breakers equipped with closing resistors, but this solution is relatively expensive.

Worst case of uncontrolled energization at peak voltage in all phases is analyzed. Figure 21 shows voltages at the end of transmission line without surge arresters in case of uncontrolled switching.

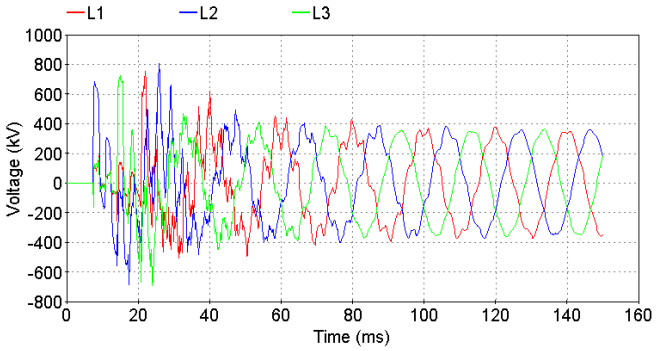

Fig. 21. Voltages at the end of transmission line without surge arresters in case of uncontrolled switching

Figure 22 depicts voltages at the end of transmission line with surge arresters U_r=342 kV in case of uncontrolled switching.

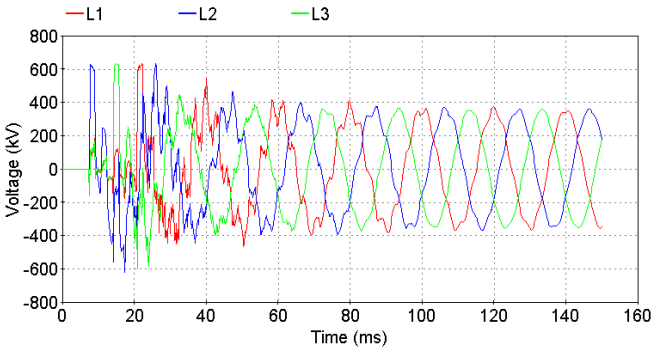

Fig. 22. Voltages at the end of transmission line with surge arresters in case of uncontrolled switching

Table III shows the comparison between uncontrolled and controlled switching regarding the amplitudes of switching overvoltages at the end of the unloaded line. It can be seen that switching overvoltages are significantly lower in case of controlled switching.

TABLE III
SWITCHING OVERVOLTAGE AMPLITUDES AT THE END OF UNLOADED LINE IN CASE OF ENERGIZATION WITHOUT TRAPPED CHARGE

	Voltage amplitude (kV)					
	Uncontrolled switching			Controlled switching		
	U_{L1}	U_{L2}	U_{L3}	U_{L1}	U_{L2}	U_{L3}
Without surge arresters	752	803	723	392	401	397
With surge arresters	634	630	632			

Controlled energization at optimum instants of circuit breaker poles closing at voltage zero-crossing is simulated. Figure 23 shows voltages at the end of the line for this case.

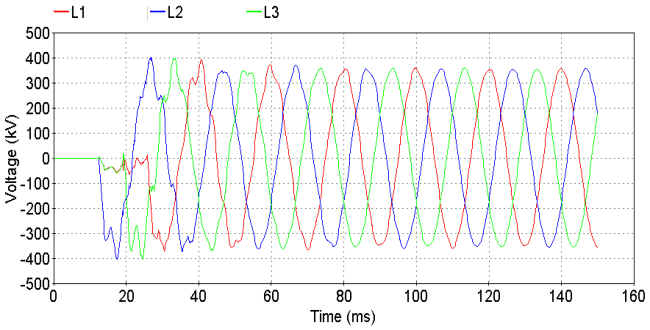

Fig. 23. Voltages at the end of transmission line in case of controlled switching

E. Auto-reclosure of unloaded 400 kV transmission line

In the case of transmission line with a capacitive potential transformers connected at both ends, no leakage path exists for the trapped charge. Figure 24 shows voltages at the end of transmission line without surge arresters in case of uncontrolled switching.

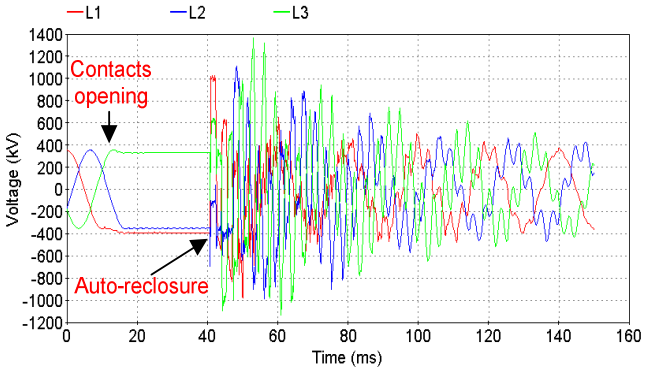

Fig. 24. Voltages at the end of transmission line without surge arresters in case of uncontrolled switching

Contact closing occurs at voltage peak on the source-side of the opposite polarity to the trapped charge. This represents the most severe case of uncontrolled auto-reclosure.

Figure 25 shows voltages at the end of transmission line with surge arresters in case of uncontrolled switching. The optimum instant of circuit breaker switching is the voltage peak on the source-side of the same polarity as the trapped charge (Fig. 26).

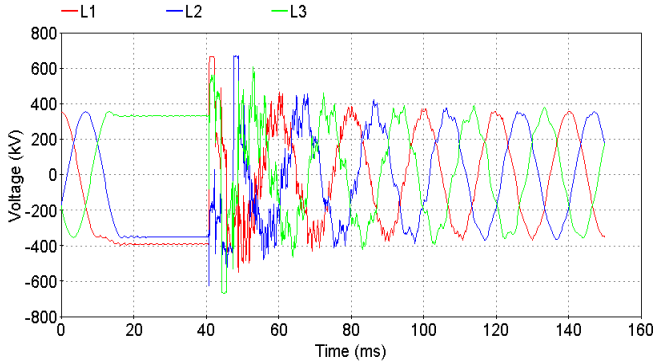

Fig. 25. Voltages at the end of transmission line with surge arresters in case of uncontrolled switching

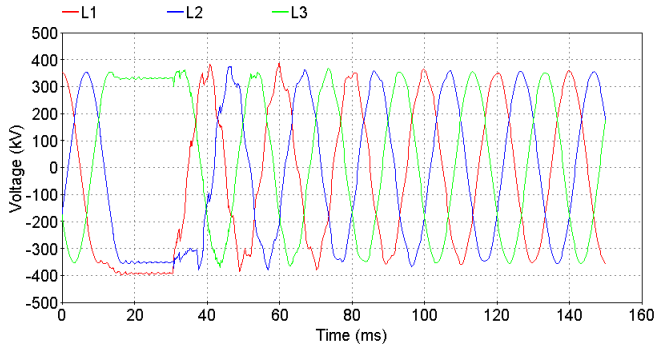

Fig. 26. Voltages at the end of transmission line in case of controlled switching

Table IV shows the comparison between uncontrolled and controlled switching regarding the amplitudes of switching overvoltages at the end of the unloaded line. It can be seen that switching overvoltages are significantly lower in case of controlled switching.

TABLE IV
SWITCHING OVERVOLTAGE AMPLITUDES AT THE END OF UNLOADED LINE IN CASE OF AUTO-RECLOSURE

	Voltage amplitude (kV)					
	Uncontrolled switching			Controlled switching		
	U_{L1}	U_{L2}	U_{L3}	U_{L1}	U_{L2}	U_{L3}
Without surge arresters	1027	1115	1363	386	375	368
With surge arresters	663	671	609			

IV. CONCLUSION

This paper describes switching transients caused by uncontrolled and controlled switching of high-voltage circuit breaker. Switching of shunt reactor and no-load transmission line was analyzed using EMTP-RV software.

Amplitudes and DC components of inrush currents and zero-sequence current are significantly lower in case of reactor controlled switching compared to uncontrolled switching.

Switching-off, energization and auto-reclosure of unloaded 400 kV transmission line was presented. Controlled switching generates significantly lower overvoltages.

As a consequence, controlled switching reduces the mechanical and electromagnetic stresses of the high voltage equipment and also prevents the unwanted operation of relay protection.

REFERENCES

[1] I. Uglešić, S. Hutter, B. Filipović-Grčić, M. Krepela, F. Jakl, "Transients Due to Switching of 400 kV Shunt Reactor", International Conference on Power System Transients (IPST), Rio de Janeiro, Brazil, June 24-28, 2001.

[2] Karcius M. C. Dantas, Washington L. A. Neves, Damásio Fernandes Jr., Gustavo A. Cardoso, Luiz C. Fonseca, "On Applying Controlled Switching to Transmission Lines: Case Studies", International Conference on Power Systems Transients (IPST), Kyoto, Japan June 3-6, 2009.

[3] CIGRE TF13.00.1, "Controlled Switching, State-of-the-Art Survey", Part 1: ELECTRA, No.162, pp. 65-96, Part 2: ELECTRA No.164, pp. 39–61, 1995.

[4] Mitsubishi Electric Advance: "Controlled Switching System", Vol.117, ISSN 1345-3041, Japan, 2007.

[5] Z. Gajić, B. Hillstrom, F. Mekić, "HV shunt reactor secrets for protection engineers", 30th Western Protective Relaying Conference, Washington, 2003

[6] EMTP-RV, documentation, WEB site www.emtp.com.

[7] Vernieri, J; Barbieri, B; Arnera P: "Influence of the representation of the distribution transformer core configuration on voltages during unbalanced operations", International Conference on Power System Transients (IPST), Rio de Janeiro, 2001.

[8] ABB, "Controlled Switching, Buyer´s & Application Guide", Edition 4, 2013.

[9] S. Bojić, I. Uglešić, B. Filipović-Grčić, "Switching Transients in 400 kV Transmission Network due to Circuit Breaker Failure", International Conference on Power Systems Transients (IPST), Vancouver, Canada, July 18-20, 2013.

[10] Ali F. Imece, D. W. Durbak, H. Elahi, S. Kolluri, A. Lux, D. Mader, T. E. McDemott, A. Morched, A. M. Mousa, R. Natarajan, L. Rugeles, and E. Tarasiewicz, "Modeling guidelines for fast front transients", Report prepared by the Fast Front Transients Task Force of the IEEE Modeling and Analysis of System Transients Working Group, *IEEE Transactions on Power Delivery*, Vol. 11, No. 1, January 1996.

[11] IEC 62271-100: High-voltage switchgear and controlgear; High-voltage alternating-current circuit-breakers, 2003.